Long non-coding RNA ZFPM2-AS1 promotes colorectal cancer progression by sponging miR-137 to regulate TRIM24

MEIHUA XIAO, ZHI LIANG and ZHIHUI YIN

Department of Anorectal Surgery, The First Affiliated Hospital of University of South China, Hengyang, Hunan 421001, P.R. China

Received March 14, 2020; Accepted October 27, 2020

DOI: 10.3892/mmr.2020.11737

Abstract. Accumulating evidence indicates that long non-coding RNAs (lncRNAs) may serve essential roles during tumorigenesis of colorectal cancer (CRC). The lncRNA ZFPM2-AS1 was observed to be involved in the progression of numerous types of cancer, such as lung adenocarcinoma and cervical cancer. The aim of the present study was to investigate the expression levels and function of ZFPM2-AS1 in CRC. Expression levels of ZFPM2-AS1 in tissue and CRC cells were measured by reverse transcription-quantitative PCR. Furthermore, cell proliferation and Transwell assays were conducted to investigate the functional role of ZFPM2-AS1 *in vitro*. In addition, bioinformatics analysis, luciferase reporter assay, RNA immunoprecipitation assay and western blotting were performed to explore the possible underlying mechanism. The expression levels of ZFPM2-AS1 were significantly upregulated in tissue samples from patients with CRC and CRC cell lines compared with normal tissue and normal human colorectal mucosa cell line. Notably, the upregulation of ZFPM2-AS1 was significantly associated with tumor size, histological differentiation, lymph node metastasis and TNM stage. In addition, ZFPM2-AS1 knockdown significantly inhibited cell proliferation, migration and invasion compared with the control group *in vitro*. Moreover, it was found that ZFPM2-AS1 positively regulated tripartite motif containing 24 (TRIM24) expression by sponging miR-137. In conclusion, the present study indicated that ZFPM2-AS1 may serve as an oncogene in CRC by regulating the miR-137/TRIM24 axis.

Introduction

Colorectal cancer (CRC) is a common digestive tract malignancy, which ranks third amongst cancer incidence rates and is the second leading cause of cancer-related death worldwide. CRC accounts for >6.1% of all malignant incidences, with ~1.8 million new CRC cases diagnosed worldwide in 2018 (1). Despite the significant progress made in CRC treatment, including in chemotherapy and surgical techniques, patients with distant metastases have a poor prognosis. Indeed, the 5-year survival rate is <10% for patients with distant metastases (2). Tumor metastasis is the primary cause of poor prognosis in patients with CRC (3). Thus, understanding the underlying molecular mechanisms associated with CRC metastasis is an urgent requirement.

Long non-coding RNAs (lncRNAs) are non-protein-encoding RNAs >200 nucleotides in length (4). A previous study indicated that lncRNAs participate in the regulation of gene expression and serve functional roles both in physiological and pathological processes (5). Furthermore, aberrant expression of lncRNAs has been implicated in tumorigenesis and the development of hepatocellular carcinoma and pancreatic ductal adenocarcinoma (6,7). For example, lncRNA SNHG6 has been reported to promote the migration, invasion and epithelial-mesenchymal transition of CRC cells through the microRNA (miRNA/miR)-26a/EZH2 axis, thereby acting as an oncogene (8). Zhan *et al* (9) reported that the overexpression of lncRNA ROR promoted the invasion and metastasis of pancreatic cancer by upregulating ZEB1 expression levels.

Kong *et al* (10) demonstrated that the recently identified lncRNA ZFPM2-AS1, located on human chromosome 8, was upregulated in gastric cancer tissue and that ZFPM2-AS1 overexpression promoted the proliferation and inhibited the apoptosis of gastric cancer cells by inhibiting the p53 pathway. Furthermore, Xue *et al* (11) indicated that ZFPM2-AS1 played an oncogenic role in lung adenocarcinoma progression through miR-18b-5p and VMA21. However, whether ZFPM2-AS1 is expressed in CRC tissue or plays a biological role in CRC progression remains unknown.

The aim of the present study was to elucidate the function of ZFPM2-AS1 in the development of CRC. This study demonstrated that ZFPM2-AS1 expression was upregulated in CRC tissues compared with normal tissue, and that high ZFPM2-AS1 expression was associated with poor prognosis for patients with CRC. Moreover, ZFPM2-AS1 knockdown inhibited the proliferation, migration and invasion of CRC cells *in vitro*. Prediction of target genes, luciferase reporter and rescue experiment assays indicated that miR-137 was a target of ZFPM2-AS1, and tripartite motif containing 24 (TRIM24) was identified as a target of miR-137. Mechanistic studies

Correspondence to: Dr Zhihui Yin, Department of Anorectal Surgery, The First Affiliated Hospital of University of South China, 69 Chuan Shan Road, Hengyang, Hunan 421001, P.R. China
E-mail: dryzh2020@163.com

Key words: colorectal cancer, ZFPM2-antisense RNA 1, progression

further clarified that ZFPM2-AS1 served as a competing endogenous RNA (ceRNA) that upregulates TRIM24 expression by sponging miR-137 in CRC.

Materials and methods

Patient tissues. Human CRC tissue samples and the matched normal tissue (n=58 pairs) were collected from The First Affiliated Hospital of the University of South China between May 2016 and March 2019. The inclusion criteria included: Patients who were diagnosed with CRC by a pathologist and underwent radical surgery. The exclusion criteria included the following: Patients had received radiotherapy or chemotherapy prior to the operation. Written informed consent was obtained from all patients. The present study was approved by the Medical Ethics Committees of The First Affiliated Hospital of University of South China.

Cell lines and culture. The human CRC cell lines (SW480, SW620, HT-29, Caco-2 and HCT116) and the normal human colorectal mucosa cell line FHC were purchased from The Cell Bank of Type Culture Collection of the Chinese Academy of Sciences. All cells were cultured in RPMI-1640 medium (Gibco; Thermo Fisher Scientific, Inc.), supplemented with 10% FBS (Gibco; Thermo Fisher Scientific, Inc.) and 1% penicillin-streptomycin (Beijing Solarbio Science & Technology Co., Ltd.) in an incubator at 37˚C with 5% CO_2.

Cell transfection. To stably knockdown the expression of ZFPM2-AS1, three short hairpin (sh) RNA targeting ZFPM2-AS1 (sh-ZFPM2-AS1-1, 5'-GCGACCTAGGATCGAACCGAT-3'; sh-ZFPM2-AS1-2, 5'-AGCTGAATTCGAGCCAATTGCGT-3'; sh-ZFPM2-AS1-3, 5'-GCCGGAACGGATTTCGGAGAC-3') and sh-negative control (NC, 5'-TTCTCCG AACGTGTCA CGT-3') were synthesized by Shanghai GenePharma Co., Ltd. These sequences were inserted into a pLKO.1 vector (BioSettia, Inc.). miR-137 mimics (5'-GUACUUCCUAACCCAUUGU UCA-3'),miR-137inhibitors(5'-AUUCUUCAGAUUUCCAGGG ACU-3'), mimics NC (5'-CAGUACUUUUGUGUAGUACAA-3') and inhibitor NC (5'-CAGUACUUUUGUGUAGUACAA-3') were also obtained from Shanghai GenePharma Co., Ltd. To construct the TRIM24 expression vector, the full-length sequence of TRIM24 were cloned into the pcDNA3.1 vector (pcDNA3.1-TRIM24). Before transfection, cells were sub-cultured into 6-well plates (Corning, Inc.) at ~50% confluence ($3x10^5$). sh-RNAs (100 nM) or miR-137 mimics (50 nM) or miR-137 inhibitor (150 nM) or plasmids (1.5 μg per well) were transfected into SW480 and HCT116 cells. Cell transfection was performed using Lipofectamine® LTX (Invitrogen; Thermo Fisher Scientific, Inc.). After incubation for 48 h, cells were collected for subsequent experiments.

RNA extraction and reverse transcription-quantitative PCR (RT-qPCR). Total RNA from CRC tissue, normal tissue, SW480 and HCT116 cells were extracted using TRIzol® reagent (Invitrogen; Thermo Fisher Scientific, Inc.). To determine mRNA and lncRNA expression levels, the extracted RNA was reverse transcribed into cDNA using a PrimeScript RT reagent kit (Takara Bio, Inc.). Reverse transcription protocol consisted of 37˚C for 15 min, followed by 85˚C for 5 sec. To determine miRNA expression levels, cDNA was synthesized using the qScript microRNA cDNA Synthesis kit (Guangzhou RiboBio Co., Ltd.). The thermocycling conditions were as follows: 94˚C for 3 min, followed by 30 cycles of 94˚C for 30 sec, 55˚C for 30 sec and 72˚C for 60 sec, and a final extension at 72˚C for 5 min. RT-qPCR was subsequently performed using SYBR-Green (Takara Bio, Inc.), GAPDH and U6 were used as the internal loading controls for lncRNA, mRNA and miRNA, respectively. The relative expression of these genes was determined using the $2^{-\Delta\Delta Cq}$ method (12).The primers used for the RT-qPCR are presented in Table I.

Cell proliferation assay. The proliferative capacity of SW480 and HCT116 cells were determined using MTS and colony formation assays. For the MTS assay, $2x10^3$ cells/well were seeded into 96-well plates and cultured for 0, 24, 48, 72, 96 and 120 h. Following the incubation, 10 μl MTS solution/well was added for 2 h, and then dimethyl sulfoxide was used to dissolve formazan. Finally, the absorbance at 450 nm was measured using a microplate reader (Bio-Rad Laboratories, Inc.).

For the colony formation assay, 800 cells/well were seeded into 6-well plates and incubated at 37˚C in 5% CO_2 for 14 days. Following the incubation, the colonies were fixed with methanol at room temperature for 10 min and stained with 0.1% crystal violet at room temperature for 10 min. The number of colonies (a single colony was defined as cell number >50) was counted using an inverted microscope (magnification, x200; CKX41; Olympus Corporation).

Transwell migration and invasion assays. Transwell assays were performed to analyze the migratory and invasive abilities of SW480 and HCT116 cells. For invasion assays, the Transwell membrane was coated with Matrigel™ (BD Biosciences) and $5x10^4$ cells/well were suspended in 200 μl serum-free medium and plated into the upper chambers. For migration assays, cells were plated in the same conditions, but the Transwell membrane was left uncoated. A volume of 750 μl medium containing 10% FBS was added to the lower chamber. Following 48 h of incubation at 37˚C with 5% CO_2, the cells were fixed with methanol at room temperature for 10 min and stained with 0.1% crystal violet at room temperature for 10 min. The stained cells were counted under an inverted microscope (magnification, x200; CKX41; Olympus Corporation).

Dual-luciferase reporter assay. The potential targets of ZFPM2-AS1 or miR-137 were predicted using miRBase 21.0 (http://www.mirbase.org/) or TargetScan 7.2 (http://www.targetscan.org/vert_72/). The sequences of the NC, wild-type (WT) ZFPM2-AS1 (ZFPM2-AS1-WT) and mutant (MUT) ZFPM2-AS1 (ZFPM2-AS1-MUT) were inserted into the pmirGLO reporter vector (Shanghai GenePharma Co., Ltd.). Subsequently, pmirGLO-NC, pmirGLO-ZFPM2-AS1-WT and pmirGLO-ZFPM2-AS1-MUT were co-transfected into SW480 and HCT116 cells along with the miR-137 mimics or miR-NC using LTX (Invitrogen; Thermo Fisher Scientific, Inc.).

Similarly, the sequences of NC, TRIM24-WT and TRIM24-MUT were inserted into the pmirGLO reporter vector. pmirGLO-NC, pmirGLO-TRIM24-WT and pmirGLO-TRIM24-MUT were then co-transfected into SW480 and HCT116 cells along with the miR-NC or miR-137 mimics with Lipofectamine 2000. Following 48 h of transfection,

Table I. Primer sequences.

Gene	Primer sequences (5'→3')
ZFPM2-AS1	F: TTTCCTACAATGAATCCACCAG
	R: TTTGAGCCACTCTTTGAGG
miR-137	F: UUAUUGCUUAAGAAUACGCGUAG
	R: GTCGTATCCAGTGCAGGGTCCGAGGT
U6	F: CTCGCTTCGGCAGCACA
	R: AACGCTTCACGAATTTGCGT
TRIM24	F: CGCCACCCAAGTTGGAGT
	R: GCTGGGAACCTCAGTAGTGTCCT
GAPDH	F: GCACCGTCAAGGCTGAGAAC
	R: GCCTTCTCCATGGTGGTGAA

miR, microRNA, TRIM24, tripartite motif containing 24; F, forward; R, reverse.

the relative luciferase activity was analyzed using the Dual Luciferase Reporter Assay System (Promega Corporation). The *Renilla* luciferase was selected as an internal control.

RNA immunoprecipitation (RIP) assay. A RIP assay was conducted to determine the interaction between ZFPM2-AS1 and miR-137 using a Magna RIP kit (EMD Millipore). Briefly, cells were lysed in RIP lysis buffer (EMD Millipore) containing magnetic beads (2 μg) conjugated with human anti-Argonaute 2 (Ago2) antibody (5 μg) (cat. no. 186733; Abcam). Input and normal IgG (EMD Millipore) were used as internal controls. Then, RT-qPCR was performed to analyze ZFPM2-AS1 and miR-137 expression levels.

Western blotting. Western blotting was performed according to a previously described study (13). Total protein was extracted with a pre-cooled RIPA lysis (cat. no. KGP703-100; Nanjing KeyGen Biotech Co., Ltd.). Protein concentration was detected with a BCA assay (Thermo Fisher Scientific, Inc.). Equal amounts (60 μg/lane) of protein aliquots were loaded on 10% gel and separated via SDS-PAGE, following which, separated proteins were transferred to PVDF membranes (EMD Millipore). Membranes were blocked with 5% skimmed milk at room temperature for 2 h, and then incubated with primary antibodies at 4˚C overnight. The following primary antibodies were used: Anti-TRIM24 (1:3,000; Abcam; cat. no. 70560) and anti-GAPDH (1:2,500; Abcam; cat. no. 9485). Subsequently, membranes were incubated with a HRP-conjugated rabbit anti-goat IgG antibody (1:10,000; cat. no. BA1060; Wuhan Boster Biological Technology, Ltd.) at room temperature for 1 h. Finally, the immunoblots were visualized with LI-COR Odyssey CLX Two-colour infrared laser imaging system (LI-COR Biosciences). ImageJ v1.8.0 software (National Institutes of Health) was used for densitometric analysis.

Statistical analysis. Statistical analysis was performed using SPSS 18.0 software (SPSS Inc.) and data are presented as the mean ± SD. A paired t-test was performed to compare expression between tumor and healthy tissues. For other comparisons between two groups, the unpaired t-test was performed. For all comparisons among ≥3 groups of data, Tukey's test was performed after one-way ANOVA analysis. The association between the clinical parameters of patients with CRC and ZFPM2-AS1 expression levels in the CRC cohort were analyzed using a χ^2 test. Pearson's correlation was used to analyze the expression levels of ZFPM2-AS1, miR137 and TRIM24. All experiments were performed in triplicate. $P<0.05$ was considered to indicate a statistically significant difference.

Results

ZFPM2-AS1 expression levels are upregulated in CRC tissue and predict an unfavorable prognosis for patients with CRC. The expression levels of ZFPM2-AS1 in 58 CRC tissue samples and matched normal tissue were analyzed by RT-qPCR. ZFPM2-AS1 expression levels were significantly upregulated in CRC tissue, compared with healthy tissue (Fig. 1A). The expression levels of ZFPM2-AS1 in the SW480, SW620, HT-29, Caco-2 and HCT116 human CRC cell lines, were also significantly upregulated, compared with FHC cells (Fig. 1B).

Subsequently, to further determine the clinical significance of ZFPM2-AS1 expression levels in CRC, patients with CRC were divided into a high expression group (n=29) and a low expression group (n=29), according to the median expression levels of ZFPM2-AS1 across all CRC tissue samples. The expression levels of ZFPM2-AS1 were positively associated with tumor size (P=0.004), histological differentiation (P=0.012), lymph node metastasis (P=0.019) and TNM stage (P=0.031) (Table II). Taken together, these results suggested that ZFPM2-AS1 could function as an oncogenic lncRNA in CRC.

ZFPM2-AS1 knockdown inhibits the proliferation, migration and invasion of CRC cells. Loss-of-function experiments were conducted to investigate the function of ZFPM2-AS1 in CRC progression. SW480 and HCT116 cells were transfected with sh-ZFPM2-AS1-1, -2 or -3 downregulate ZFPM2-AS1 expression. sh-ZFPM2-AS1-1 used in subsequent experiments, due to its superior knockdown efficiency (Fig. 1C), compared with the other two shRNA candidates.

MTS and colony formation assays demonstrated that ZFPM2-AS1-1 knockdown significantly inhibited the proliferative ability of CRC cells (Fig. 1D and E), compared with sh-NC. In addition, Transwell assays indicated that the migratory and invasive abilities of CRC cells transfected with sh-ZFPM2-AS1 were markedly decreased (Fig. 1F). Thus, ZFPM2-AS1-1 knockdown may lead to significant inhibition of the proliferation, migration and invasion of CRC cells.

ZFPM2-AS1 serves as a sponge for miR-137. To further identify the underlying mechanisms of ZFPM2-AS1 in CRC progression, miRBase was used to predict potential target miRNAs for ZFPM2-AS1. Thus, miR-137 was identified as a candidate target of ZFPM2-AS1 (Fig. 2A). Following ZFPM2-AS1 knockdown, miR-137 expression levels were significantly upregulated, compared with sh-NC (Fig. 2B). miR-137 mimics and inhibitor, as well as their respective NC were then transfected into SW480 and HCT116 cell lines. The expression of miR-137 was significantly upregulated in miR-137 mimics-transfected cells, whereas

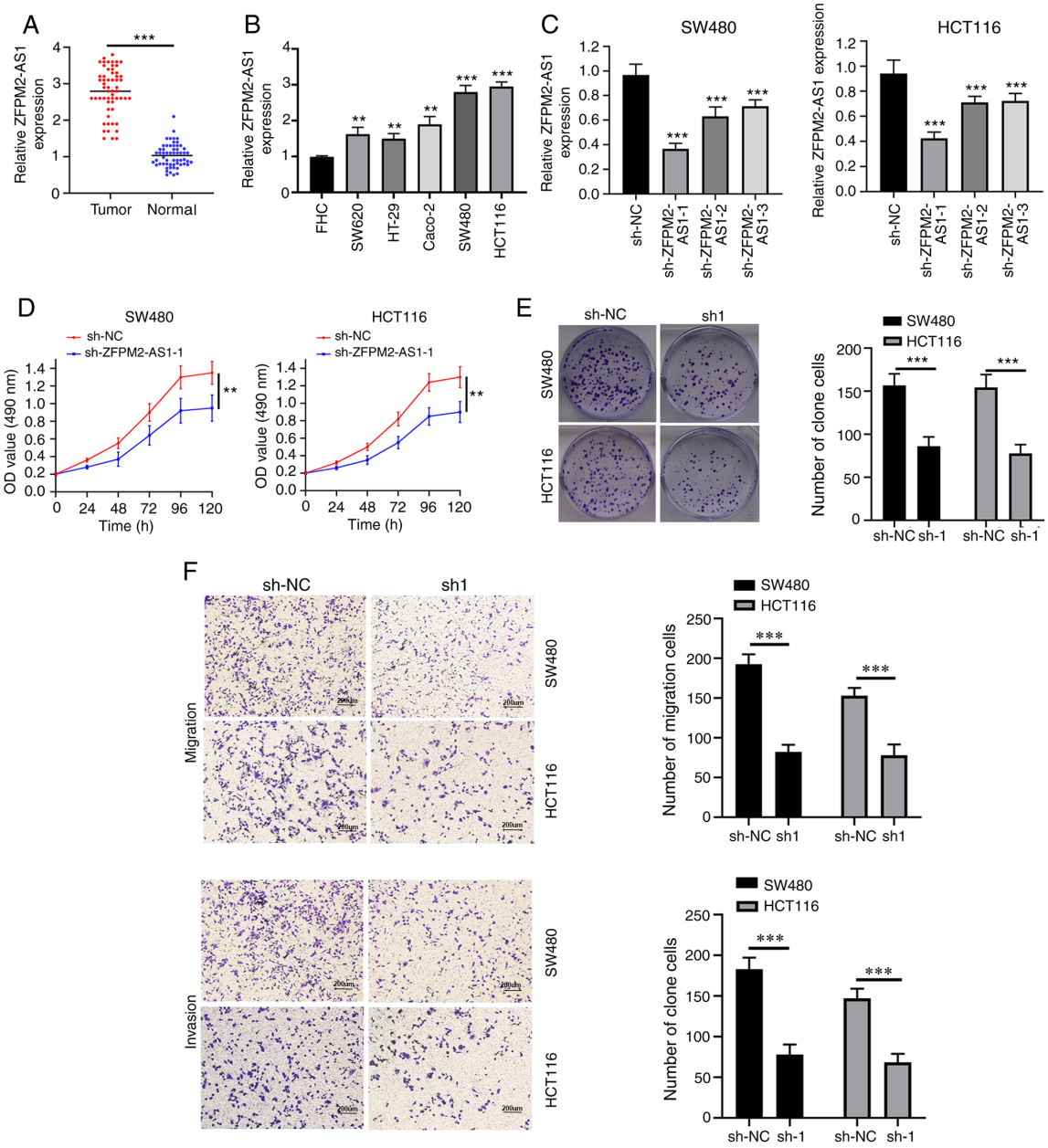

Figure 1. ZFPM2-AS1 knockdown attenuates the proliferation, migration and invasion of CRC cells. (A) ZFPM2-AS1 expression in CRC tumor tissues and in adjacent normal tissues. (B) ZFPM2-AS1 mRNA expression in CRC cell lines. (C) ZFPM2-AS1 expression in SW480 and HCT116 cells stably expressing sh-NC or sh-ZFPM2-AS1. (D and E) Effects of sh-ZFPM2-AS1 on cell proliferation of SW480 and HCT116 cells. (F) Effects of sh-ZFPM2-AS1 on cell migration and invasion of SW480 and HCT116 cells (scale bar, 200 μm). **P<0.01, ***P<0.001 vs. control group. CRC, colorectal cancer; sh, short hairpin; NC, negative control; OD, optical density.

miR-137 expression was significantly decreased in miR-137 inhibitor-transfected cells, compared with their NC (Fig. 2C). The miR mimics and mimics NC were then used in dual-luciferase reporter assays. Co-transfection with miR-137 mimics significantly decreased the relative luciferase activity of ZFPM2-AS1-WT, but not MUT, compared with mimics-NC (Fig. 2D).

In a RIP assay, both ZFPM2-AS1 and miR-137 were significantly enriched in Ago2-containing beads, compared with the IgG-containing beads (Fig. 2E). Furthermore, the relative expression levels of miR-137 were significantly downregulated in CRC tissue compared with matched normal tissue (Fig. 2F). The expression levels of miR-137 were significantly downregulated in CRC cell lines (SW620, HT-29, Caco-2, SW480 and HCT116) compared with FHC cells (Fig. 2G). In addition, miR-137 expression levels were negatively correlated with ZFPM2-AS1 expression in CRC tissue (Fig. 2H). Notably, co-transfection of SW480 and HCT116 cells with miR-137 inhibitor and sh-ZFPM2-AS1-1 significantly increased cell proliferation, migration and invasion abilities, compared with shRNA alone (Fig. 2I-K). These results suggested that ZFPM2-AS1 may promote CRC progression by sponging miR-137.

miR-137 targets TRIM24 in CRC. TargetScan7 was used to predict the downstream targets of miR-137, which identified TRIM24 as a potential candidate gene (Fig. 3A). TRIM24 mRNA expression levels were significantly upregulated in CRC tissues compared with the adjacent normal tissues (Fig. 3B). Moreover, TRIM24 mRNA levels were significantly upregulated

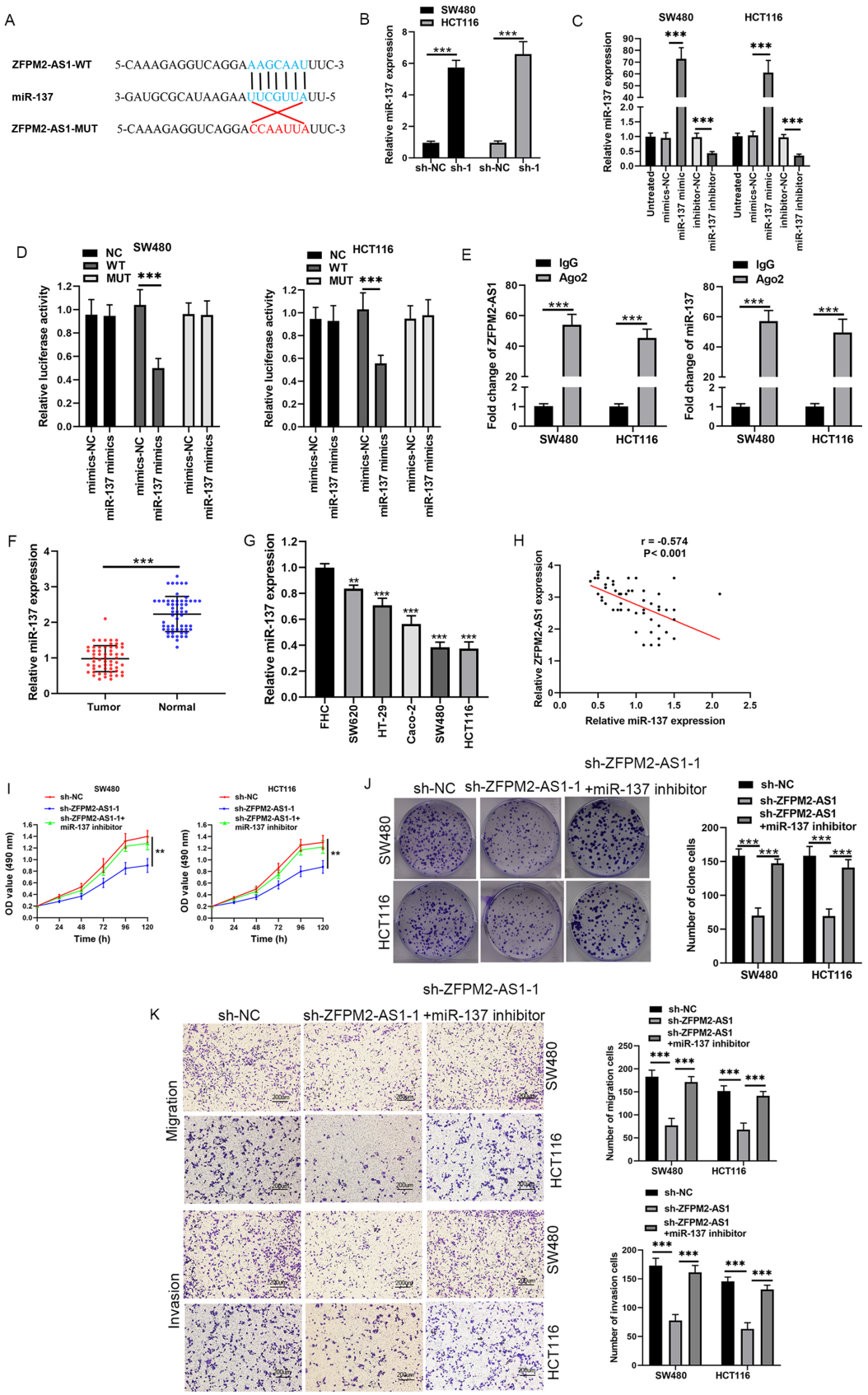

Figure 2. miR-137 is a direct target of ZFPM2-AS1. (A) Predicted binding site of miR-137 in ZFPM2-AS1. (B) miR-137 expression in SW480 and HCT116 cells transfected with sh-ZFPM2-AS1. (C) miR-137 expression in SW480 and HCT116 cells following transfection with miR-137 mimics or miR-137 inhibitor. (D) Effects of miR-137 mimics on luciferase activity WT or MUT ZFPM2-AS1 gene constructs. (E) Radioimmunoprecipitation and reverse transcription-quantitative PCR analysis of the binding between ZFPM2-AS1 and miR-137. (F) miR-137 expression in CRC tumor tissues and in adjacent normal tissues. (G) miR-137 expression in CRC cell lines. (H) Correlation between ZFPM2-AS1 and miR-137 expressions in CRC tissues. (I and J) Effects of sh-ZFPM2-AS1 and miR-137 inhibitor on proliferation of SW480 and HCT116 cells. (K) Effects of sh-ZFPM2-AS1 and miR-137 inhibitor on cell migration and invasion of SW480 and HCT116 cells (scale bar, 200 μm). **P<0.01, ***P<0.001 vs. control group. miR, microRNA; CRC, colorectal cancer; sh, short hairpin; NC, negative control; OD, optical density; WT, wild-type; MUT, mutant; Ig, immunoglobulin; Ago2, Argonaute 2.

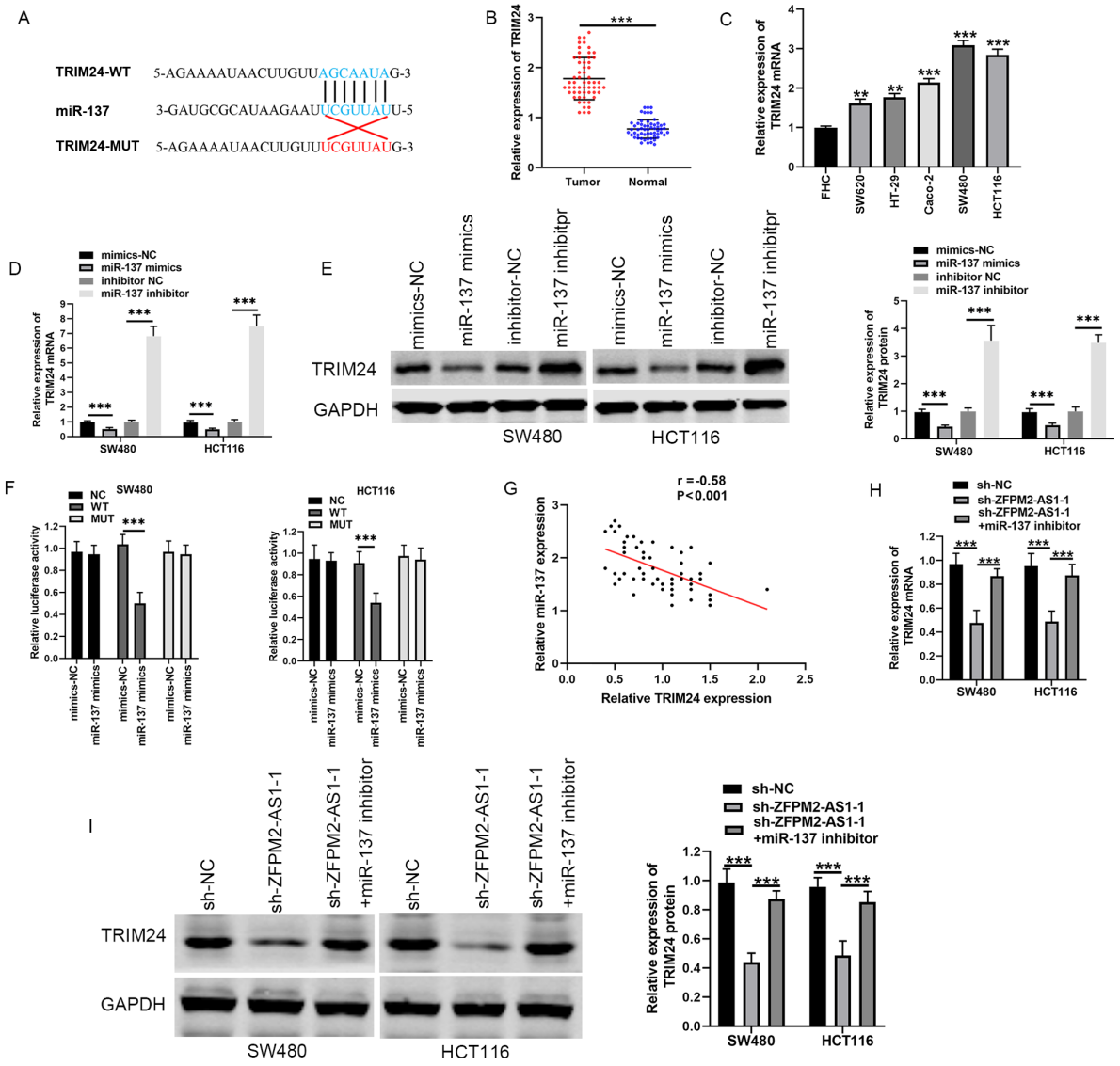

Figure 3. TRIM24 is a direct target of miR-137. (A) Predicted binding site of miR-137 in TRIM24. (B) TRIM24 mRNA expression in CRC tumor and adjacent normal tissue. (C) TRIM24 mRNA expression in CRC cell lines. (D) TRIM24 mRNA and (E) protein expression following transfection with miR-137 mimics or miR-137 inhibitor in SW480 and HCT116 cells. (F) Effects of miR-137 mimics on luciferase activity of WT or MUT TRIM24 constructs. (G) Correlation between TRIM24 and miR-137 expressions in CRC tissues. (H) TRIM24 mRNA and (I) protein expression following transfection with sh-ZFPM2-AS1 and miR-137 inhibitor in SW480 and HCT116 cells. **P<0.01, ***P<0.001 vs. control group. miR, microRNA; CRC, colorectal cancer; TRIM24, tripartite motif containing 24; sh, short hairpin; NC, negative control; WT, wild-type; MUT, mutant.

in CRC cell lines (SW620, HT-29, Caco-2, SW480 and HCT116), compared with FHC cells (Fig. 3C). The effects of miR-137 mimics and miR-137 inhibitor on TRIM24 mRNA and protein expression in CRC cells were then evaluated. Compared with mimics NC, TRIM24 expression was significantly decreased both at the mRNA and protein levels in CRC cells transfected with miR-137 mimics. By contrast, the miR-137 inhibitor increased the expression levels of TRIM24 (Fig. 3D and E). In a dual-luciferase reporter assay, miR-137 mimics significantly inhibited the relative luciferase activity of TRIM24-WT, but not TRIM24-MUT (Fig. 3F). Pearson's correlation analysis also indicated that miR-137 expression levels were negatively correlated with TRIM24 expression levels in CRC tissues (Fig. 3G).

RT-qPCR and western blot analysis were then carried out to determine whether ZFPM2-AS1 could regulate TRIM24 expression levels. TRIM24 expression levels were significantly downregulated following ZFPM2-AS1 knockdown. However, transfection with the miR-137 inhibitor and sh-ZFPM2-AS1-1 increased the expression levels of TRIM24, compared with shRNA alone (Fig. 3H and I). Thus, ZFPM2-AS1 may promote TRIM24 expression by sponging miR-137 in CRC.

ZFPM2-AS1 promotes CRC progression through TRIM24. To determine whether ZFPM2-AS1 promoted CRC progression through TRIM24, RT-qPCR and western blotting analyses were carried out following TRIM24 overexpression. TRIM24 expression was significantly increased after transfection with pcDNA3.1-TRIM24 (Fig. 4A). Compared with sh-NC and TRIM24 overexpression, ZFPM2-AS1 knockdown significantly downregulated TRIM24 expression levels, both at the mRNA and protein level (Fig. 4B and C). Pearson's correlation analysis indicated that TRIM24 expression levels were positively correlated with ZFPM2-AS1 expression levels in CRC tissue (Fig. 4D). Moreover, proliferation, migration and

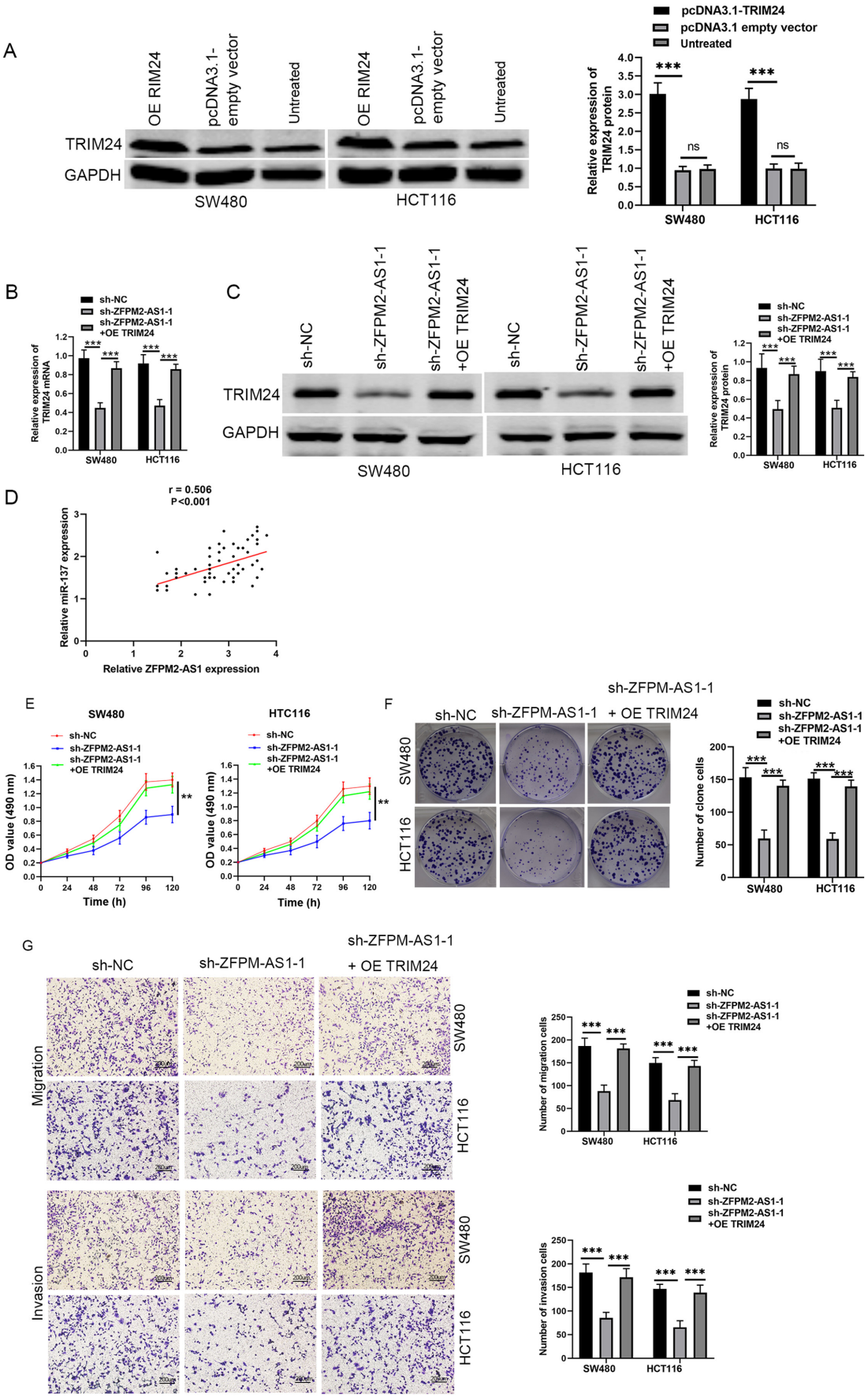

Figure 4. TRIM24 overexpression reverses the effects of ZFPM2-AS1 knockdown in CRC cell lines. (A) Effects of pcDNA3.1-TRIM24 on TRIM24 protein expression in SW480 and HCT116 cells. (B) TRIM24 mRNA and (C) protein expression in SW480 and HCT116 cells transfected with sh-ZFPM2-AS1 and pcDNA3.1-TRIM24. (D) Correlation between TRIM24 and ZFPM2-AS1 expressions in CRC tissue. (E and F) Effects of sh-ZFPM2-AS1 and pcDNA3.1-TRIM24 on proliferation of SW480 and HCT116 cells. (G) Effects of sh-ZFPM2-AS1 and pcDNA3.1-TRIM24 on cell migration and invasion of HCT116 and SW480 cells. **P<0.01, ***P<0.001. CRC, colorectal cancer; TRIM24, tripartite motif containing 24; sh, short hairpin; NC, negative control; OE, overexpression.

Table II. Association between ZFPM2-AS1 expression and clinicopathological characteristics of patients with colorectal cancer.

		ZFPM2-AS1 expression			
Clinicopathological characteristics	Cases, n	Low, n	High, n	χ^2 value	P-value
Age, years					
<60	23	11	12	0.232	0.630
≥60	35	19	16		
Sex					
Male	31	15	16	0.297	0.586
Female	27	15	12		
Tumor size, cm					
<5	28	20	8	8.417	0.004
≥5	30	10	20		
Differentiation					
Good/moderate	22	16	6	6.262	0.012
Poor	36	14	22		
Lymph node metastasis					
No	19	14	5	5.457	0.019
Yes	39	16	23		
TNM stage					
I+II	25	17	8	6.661	0.031
III+IV	33	13	20		

invasion of CRC cell lines were significantly inhibited by ZFPM2-AS1 silencing, which was partly reversed following TRIM24 overexpression (Fig. 4E-G). Taken together, these findings suggested that ZFPM2-AS1 may serve an oncogenic role in CRC through a miR-137/TRIM24 axis.

Discussion

Accumulating evidence suggests that lncRNAs exert pivotal functions in the development and progression of CRC. For example, Gao *et al* (14) reported that the upregulation of lncRNA CACS15 contributed to oxaliplatin resistance of CRC by regulating the miR-145/ABCC1 axis. Xu *et al* (15) demonstrated that lncRNA MALAT1 promoted CRC cell proliferation, invasion and migration by upregulating SOX9 expression. Xu *et al* (16) reported that the expression levels of the lncRNA SATB2-AS1 were downregulated in CRC; clinical analysis indicated that low SATB2-AS1 expression levels were associated with poor prognosis. Functional analysis also demonstrated that SATB2-AS1 knockdown enhanced migration and invasion of CRC cells (16).

In the present study, the expression levels of ZFPM2-AS1 were upregulated in human CRC tissues. In addition, there was an association between ZFPM2-AS1 expression levels and clinical characteristics. Indeed, high expression levels of ZFPM2-AS1 were significantly associated with tumor size, histological differentiation, lymph node metastasis and TNM stage. Thus, it was hypothesized that ZFPM2-AS1 may serve as oncogenic role in CRC. ZFPM2-AS1 expression levels were also markedly upregulated in CRC cell lines, compared with a colorectal mucosa cell line. Furthermore, loss-of-function experiments suggested that ZFPM2-AS1 knockdown decreased SW480 and HCT116 cell proliferation, migration and invasion *in vitro*.

Previous studies have demonstrated that lncRNAs function as ceRNA networks that sponge miRNAs and modulate the expression of target mRNA molecules, resulting in changes in the progression of multiple types of cancer, such as lung adenocarcinoma and pancreatic ductal adenocarcinoma (17,18). Thus, the potential miRNAs that can bind with ZFPM2-AS1 were examined in the present study, and miR-137 was identified as a potential target. miR-137 has previously been identified as a tumor suppressor in numerous types of cancer. For example, Chen *et al* (19) reported that miR-137 expression levels were downregulated in glioblastoma, and that the overexpression of miR-137 markedly suppressed the proliferation and invasion of glioma cell lines. In addition, Li *et al* (20) demonstrated that miR-137 induced the apoptosis of ovarian cancer cells by regulating X-linked inhibitor of apoptosis protein. miR-137 also inhibits the malignant phenotype of malignant melanoma (21), tongue squamous carcinoma (22), cervical cancer (23) and CRC (24). In the present study, miR-137 could directly bind ZFPM2-AS1. Moreover, miR-137 expression levels were upregulated following ZFPM2-AS1 knockdown, and ZFPM2-AS1 expression was inversely correlated with that of miR-137 in patients with CRC. Moreover, transfection with a miR-137 inhibitor reversed the effects of ZFPM2-AS1 knockdown in CRC cells.

The downstream targets of this ZFPM2-AS1/miR-137 axis were also examined. TRIM24 was predicted as a potential target of miR-137. In a dual-luciferase reporter assay, miR-137 could directly bind to TRIM24. Moreover, TRIM24 expression levels were downregulated following the transfection with miR-137 mimics. Several previous studies have suggested that TRIM24 may serve as an oncogene in the development of several types of cancer. For instance, Zhang *et al* (25) reported that TRIM24 promoted glioma progression by enhancing the PI3K/AKT signaling pathway. Lv *et al* (26) also demonstrated that TRIM24 contributed to human glioblastoma development. In addition, Zhu *et al* (27) indicated that TRIM24 was highly expressed in human hepatocellular carcinoma (HCC) and that TRIM24 knockdown suppressed the proliferative and migratory abilities of HCC cells.

Notably, a previous study also suggested that TRIM24 expression levels were significantly upregulated in CRC tissues, compared with normal tissues, and that TRIM24 upregulation was associated with poor prognosis in patients (28). Additionally, Wang *et al* (29) reported that TRIM24 silencing inhibited the proliferation and promoted the apoptosis of CRC cells. These previous studies suggested that TRIM24 may serve as an oncogene in human CRC. Thus, it was investigated whether TRIM24 participated in the miR-137/TRIM24 axis in CRC cells. It was identified that ZFPM2-AS1 silencing downregulated TRIM24 expression levels by binding to miR-137. In addition, TRIM24 overexpression could rescue the effects of ZFPM2-AS1 knockdown on CRC cell proliferation, migration and invasion.

In conclusion, the findings of the present study suggested an important role for ZFPM2-AS1 in the proliferation, migration and invasion of CRC cells. These results also identified a novel mechanism through which the ZFPM2-AS1/miR-137/TRIM24 axis may regulate the progression of CRC.

Acknowledgements

Not applicable.

Funding

No funding was received.

Availability of data and materials

All datasets used and/or analyzed during the current study are available from the corresponding author on reasonable request.

Authors' contributions

MX and ZY carried out the study design and drafted the manuscript. MX and ZL performed the experiments. ZY conceived the study and revised the manuscript. All authors read and approved the final manuscript.

Ethics approval and consent to participate

The present study was approved by the Medical Ethics Committee of The First Affiliated Hospital of University of South China (approval no. LL20170326021). Written informed consent was obtained from all patients.

Patient consent for publication

Not applicable.

Competing interests

The authors declare that they have no competing interests.

References

1. Bray F, Ferlay J, Soerjomataram I, Siegel RL, Torre LA and Jemal A: Global cancer statistics 2018: GLOBOCAN estimates of incidence and mortality worldwide for 36 cancers in 185 countries. CA Cancer J Clin 68: 394-424, 2018.
2. Zhang J, Jiang Y, Zhu J, Wu T, Ma J, Du C, Chen S, Li T, Han J and Wang X: Overexpression of long non-coding RNA colon cancer-associated transcript 2 is associated with advanced tumor progression and poor prognosis in patients with colorectal cancer. Oncol Lett 14: 6907-6914, 2017.
3. Simon K: Colorectal cancer development and advances in screening. Clin Interv Aging 11: 967-976, 2016.
4. Bach DH and Lee SK: Long noncoding RNAs in cancer cells. Cancer Lett 419: 152-166, 2018.
5. Quinn JJ and Chang HY: Unique features of long non-coding RNA biogenesis and function. Nat Rev Genet 17: 47-62, 2016.
6. Huang JL, Cao SW, Ou QS, Yang B, Zheng SH, Tang J, Chen J, Hu YW, Zheng L and Wang Q: The long non-coding RNA PTTG3P promotes cell growth and metastasis via up-regulating PTTG1 and activating PI3K/AKT signaling in hepatocellular carcinoma. Mol Cancer 17: 93, 2018.
7. Zheng S, Chen H, Wang Y, Gao W, Fu Z, Zhou Q, Jiang Y, Lin Q, Tan L, Ye H, *et al*: Long non-coding RNA LOC389641 promotes progression of pancreatic ductal adenocarcinoma and increases cell invasion by regulating E-cadherin in a TNFRSF10A-related manner. Cancer Lett 371: 354-365, 2016.
8. Zhang M, Duan W and Sun W: LncRNA SNHG6 promotes the migration, invasion, and epithelial-mesenchymal transition of colorectal cancer cells by miR-26a/EZH2 axis. OncoTargets Ther 12: 3349-3360, 2019.
9. Zhan HX, Wang Y, Li C, Xu JW, Zhou B, Zhu JK, Han HF, Wang L, Wang YS and Hu SY: LincRNA-ROR promotes invasion, metastasis and tumor growth in pancreatic cancer through activating ZEB1 pathway. Cancer Lett 374: 261-271, 2016.
10. Kong F, Deng X, Kong X, Du Y, Li L, Zhu H, Wang Y, Xie D, Guha S, Li Z, *et al*: ZFPM2-AS1, a novel lncRNA, attenuates the p53 pathway and promotes gastric carcinogenesis by stabilizing MIF. Oncogene 37: 5982-5996, 2018.
11. Xue M, Tao W, Yu S, Yan Z, Peng Q, Jiang F and Gao X: lncRNA ZFPM2-AS1 promotes proliferation via miR-18b-5p/VMA21 axis in lung adenocarcinoma. J Cell Biochem 121: 313-321, 2020.
12. Livak KJ and Schmittgen TD: Analysis of relative gene expression data using real-time quantitative PCR and the 2(-Delta Delta C(T)) method. Methods 25: 402-408, 2001.
13. Duan X, Kong Z, Liu Y, Zeng Z, Li S, Wu W, Ji W, Yang B, Zhao Z and Zeng G: β-Arrestin2 contributes to cell viability and proliferation via the down-regulation of FOXO1 in castration-resistant prostate cancer. J Cell Physiol 230: 2371-2381, 2015.
14. Gao R, Fang C, Xu J, Tan H, Li P and Ma L: LncRNA CACS15 contributes to oxaliplatin resistance in colorectal cancer by positively regulating ABCC1 through sponging miR-145. Arch Biochem Biophys 663: 183-191, 2019.
15. Xu Y, Zhang X, Hu X, Zhou W, Zhang P, Zhang J, Yang S and Liu Y: The effects of lncRNA MALAT1 on proliferation, invasion and migration in colorectal cancer through regulating SOX9. Mol Med 24: 52, 2018.
16. Xu M, Xu X, Pan B, Chen X, Lin K, Zeng K, Liu X, Xu T, Sun L, Qin J, *et al*: LncRNA SATB2-AS1 inhibits tumor metastasis and affects the tumor immune cell microenvironment in colorectal cancer by regulating SATB2. Mol Cancer 18: 135, 2019.
17. Ge X, Li GY, Jiang L, Jia L, Zhang Z, Li X, Wang R, Zhou M, Zhou Y, Zeng Z, *et al*: Long noncoding RNA CAR10 promotes lung adenocarcinoma metastasis via miR-203/30/SNAI axis. Oncogene 38: 3061-3076, 2019.
18. Yang H, Liu P, Zhang J, Peng X, Lu Z, Yu S, Meng Y, Tong WM and Chen J: Long noncoding RNA MIR31HG exhibits oncogenic property in pancreatic ductal adenocarcinoma and is negatively regulated by miR-193b. Oncogene 35: 3647-3657, 2016.
19. Chen L, Wang X, Wang H, Li Y, Yan W, Han L, Zhang K, Zhang J, Wang Y, Feng Y, *et al*: miR-137 is frequently down-regulated in glioblastoma and is a negative regulator of Cox-2. Eur J Cancer 48: 3104-3111, 2012.
20. Li X, Chen W, Zeng W, Wan C, Duan S and Jiang S: microRNA-137 promotes apoptosis in ovarian cancer cells via the regulation of XIAP. Br J Cancer 116: 66-76, 2017.
21. Peres J, Kwesi-Maliepaard EM, Rambow F, Larue L and Prince S: The tumour suppressor, miR-137, inhibits malignant melanoma migration by targetting the TBX3 transcription factor. Cancer Lett 405: 111-119, 2017.
22. Sun L, Liang J, Wang Q, Li Z, Du Y and Xu X: MicroRNA-137 suppresses tongue squamous carcinoma cell proliferation, migration and invasion. Cell Prolif 49: 628-635, 2016.
23. Miao H, Wang N, Shi LX, Wang Z and Song WB: Overexpression of mircoRNA-137 inhibits cervical cancer cell invasion, migration and epithelial-mesenchymal transition by suppressing the TGF-β/smad pathway via binding to GREM1. Cancer Cell Int 19: 147, 2019.
24. Balaguer F, Link A, Lozano JJ, Cuatrecasas M, Nagasaka T, Boland CR and Goel A: Epigenetic silencing of miR-137 is an early event in colorectal carcinogenesis. Cancer Res 70: 6609-6618, 2010.
25. Zhang LH, Yin AA, Cheng JX, Huang HY, Li XM, Zhang YQ, Han N and Zhang X: TRIM24 promotes glioma progression and enhances chemoresistance through activation of the PI3K/Akt signaling pathway. Oncogene 34: 600-610, 2015.
26. Lv D, Li Y, Zhang W, Alvarez AA, Song L, Tang J, Gao WQ, Hu B, Cheng SY and Feng H: TRIM24 is an oncogenic transcriptional co-activator of STAT3 in glioblastoma. Nat Commun 8: 1454, 2017.
27. Zhu Y, Zhao L, Shi K, Huang Z and Chen B: TRIM24 promotes hepatocellular carcinoma progression via AMPK signaling. Exp Cell Res 367: 274-281, 2018.
28. Wang FQ, Han Y, Yao W and Yu J: Prognostic relevance of tripartite motif containing 24 expression in colorectal cancer. Pathol Res Pract 213: 1271-1275, 2017.
29. Wang J, Zhu J, Dong M, Yu H, Dai X and Li K: Knockdown of tripartite motif containing 24 by lentivirus suppresses cell growth and induces apoptosis in human colorectal cancer cells. Oncol Res 22: 39-45, 2014.